Arabidopsis protein arginine methyltransferase 3 is required for ribosome biogenesis by affecting precursor ribosomal RNA processing

Runlai Hang[a,b], Chunyan Liu[a], Ayaz Ahmad[a,b,1], Yong Zhang[a,b,2], Falong Lu[a,b,3], and Xiaofeng Cao[a,c,4]

[a]State Key Laboratory of Plant Genomics and National Center for Plant Gene Research, Institute of Genetics and Developmental Biology, Chinese Academy of Sciences, Beijing 100101, China; [b]College of Life Sciences, University of the Chinese Academy of Sciences, Beijing 100039, China; and [c]Collaborative Innovation Center for Genetics and Development, Fudan University, Shanghai 200433, China

Edited by James A. Birchler, University of Missouri-Columbia, Columbia, MO, and approved September 29, 2014 (received for review July 9, 2014)

Ribosome biogenesis is a fundamental and tightly regulated cellular process, including synthesis, processing, and assembly of rRNAs with ribosomal proteins. Protein arginine methyltransferases (PRMTs) have been implicated in many important biological processes, such as ribosome biogenesis. Two alternative precursor rRNA (pre-rRNA) processing pathways coexist in yeast and mammals; however, how PRMT affects ribosome biogenesis remains largely unknown. Here we show that *Arabidopsis* PRMT3 (AtPRMT3) is required for ribosome biogenesis by affecting pre-rRNA processing. Disruption of *AtPRMT3* results in pleiotropic developmental defects, imbalanced polyribosome profiles, and aberrant pre-rRNA processing. We further identify an alternative pre-rRNA processing pathway in *Arabidopsis* and demonstrate that AtPRMT3 is required for the balance of these two pathways to promote normal growth and development. Our work uncovers a previously unidentified function of PRMT in posttranscriptional regulation of rRNA, revealing an extra layer of complexity in the regulation of ribosome biogenesis.

arginine methylation | protein arginine methyltransferase | AtPRMT3 | ribosome biogenesis | rRNA processing

The fundamental, complicated, and highly cooperative process of ribosome biogenesis involves ribosomal DNA (rDNA) transcription, precursor rRNA (pre-rRNA) processing, and assembly with ribosomal proteins and related assembly factors (1, 2). As a multistep, error prone, and energy-consuming process, ribosome biogenesis is also highly regulated (3, 4). In eukaryotic cells, mutations in ribosomal proteins or ribosome assembly factors usually lead to aberrant pre-rRNA processing (5–7) and activation of the polyadenylation-mediated RNA quality control system (4, 8, 9), resulting in various genetic diseases in humans (10, 11).

Work in budding yeast, *Saccharomyces cerevisiae*, has deciphered the mechanisms of ribosome biogenesis (1, 2, 12). After transcription by RNA polymerase I and site-specific modification by small nucleolar ribonucleoproteins, the nascent 35S rRNA, the common precursor of 18S, 5.8S, and 25S rRNAs, is quickly assembled with many assembly factors and ribosomal proteins into small subunit processome/90S preribosomal particles (13–15). Then it mainly undergoes the "U3-dependent cleavage occurs first" pathway, which first removes the 5′ external transcribed sequence (5′ ETS) of 35S rRNA, to generate the 32S rRNA (16, 17). Next, after cleavage at the A2 site of intergenic transcribed sequence 1 (ITS1) between 18S rRNA and 5.8S rRNA, the 90S preribosomal particle splits into two independent complexes of pre-40S and pre-60S ribosomal particles. Finally, ribosomal subunits are further matured and assembled into 80S ribosomes for translation in the cytoplasm (12). However, in contrast to budding yeast, pre-rRNA processing in *Xenopus laevis* oocytes, mouse cells, and human cells preferentially cleave in ITS1 before the complete removal of the 5′ ETS (18–21), which may represent a common pathway in metazoans.

In plants, a pre-rRNA processing pathway has been described in *Arabidopsis* (22). The cleavage at A3 in ITS1 occurs before complete removal of the 5′ ETS, generating diagnostic intermediates of P-A3 (22-25) and P'-A3 fragments (23, 25) in wild type. However, it remains unknown whether *Arabidopsis* has an alternative pre-rRNA processing pathway marked by 32S rRNA, resembling the "U3 dependent cleavage occurs first" pathway in budding yeast (17, 26).

Protein arginine methyltransferases (PRMTs) catalyze the formation of methylarginines, a general posttranslational modification of proteins that occurs widely in eukaryotes (27, 28). PRMT family members have been implicated in many essential biological processes, including ribosome biogenesis at the level of ribosome assembly (29–31). Arginine methylation of the ribosomal proteins RPS3 and RPS10 in human cells, catalyzed by PRMT1 and PRMT5, respectively, facilitates their proper assembly into the ribosome small subunit (32, 33). Studies in fission yeast have emphasized the role of PRMT3 in the homeostasis of cellular ribosomal subunits. PRMT3 is a cytoplasmic protein widely expressed in eukaryotes, except budding yeast and

Significance

The functional relationship between protein arginine methyltransferases (PRMTs) and ribosome biogenesis was proposed a decade ago, but the underlying mechanism still remains elusive. In this work, we demonstrate for the first time to our knowledge that the coexistence of two pre-rRNA processing pathways is conserved in plants; and *Arabidopsis* PRMT3 is required for the balance between these pathways. These findings uncover an important link between PRMT and proper pre-rRNA processing, which not only extends our understanding of the regulatory scope of PRMTs but also reveals the complexity of regulation of ribosome biogenesis. The alternative pre-rRNA processing pathways in plants modulated by PRMT3 may be conserved in other multicellular organisms, thereby shedding light on PRMT functions and regulation of ribosome biogenesis in animals.

Author contributions: R.H., C.L., and X.C. designed research; R.H., C.L., A.A., Y.Z., and F.L. performed research; R.H., C.L., and X.C. analyzed data; and R.H. and X.C. wrote the paper.

The authors declare no conflict of interest.

This article is a PNAS Direct Submission.

Freely available online through the PNAS open access option.

[1]Present address: Department of Biotechnology, Abdul Wali Khan University, Mardan 23200, Pakistan.

[2]Present address: Department of Systems Biology, Columbia University, New York, NY 10032.

[3]Present address: Program in Cellular and Molecular Medicine, Boston Children's Hospital, Boston, MA 02115.

[4]To whom correspondence should be addressed. Email: xfcao@genetics.ac.cn.

This article contains supporting information online at www.pnas.org/lookup/suppl/doi:10.1073/pnas.1412697111/-/DCSupplemental.

Caenorhabditis elegans (30, 34, 35). PRMT3 contains a unique C2H2 (Cys2His2)-type zinc finger in the N terminus, before the catalytic core (36). The *prmt3* null mice displayed reduced embryo size, depicting *Minute*-like characteristics during organogenesis and fetal growth (37). Perturbation of *PRMT3* expression in cultured rat hippocampal neurons caused deformed spines (38). Deletion of *PRMT3* results in a striking accumulation of free 60S ribosomal subunits and decreased free 40S:60S stoichiometry (34). However, rRNA pulse-chase analysis and Northern blot assays ruled out a function of PRMT3 in pre-rRNA processing in fission yeast (34). It is still unclear whether PRMT3 affects pre-rRNA processing in higher organisms.

In this work we show that the *Arabidopsis* PRMT3 (AtPRMT3) is a conserved cytoplasm-localized active arginine methyltransferase. Null alleles of *atprmt3* exhibit pleiotropic developmental defects, imbalanced polyribosome profiles, and altered resistance to aminoglycoside antibiotics. Intriguingly, we identified the existence of 32S rRNA, which is a marker of a potential minor alternative pre-rRNA processing pathway, in wild-type Col and show it is strikingly up-regulated in *atprmt3* mutants. In contrast, the P-A3 fragment, which is a marker of the major pre-rRNA processing pathway, is down-regulated in *atprmt3* mutants. In addition, the 18S-A3 and 27SB intermediates accumulated in the *atprmt3* mutants. Taking these results together, we have uncovered an alternative pre-rRNA processing pathway in plants and shown that PRMT3 in *Arabidopsis* participates in ribosome biogenesis by modulating the balance of alternative pre-rRNA processing pathways. This function differs from its homolog in fission yeast and has not yet been characterized in mammalian systems. Our findings reveal an important link between PRMT and proper pre-rRNA processing.

Results

AtPRMT3 Is a Unique and Evolutionarily Conserved PRMT. AtPRMT3 (encoded by At3g12270), shares 33% and 34% amino acid sequence identity with its homologs, RMT3 in fission yeast and PRMT3 in rat, respectively (Fig. S1 *A* and *B*) (39). AtPRMT3 contains all of the highly conserved PRMT motifs (Fig. S1*B*). Notably, unlike other PRMTs, AtPRMT3 has a C2H2-type zinc finger unique to the PRMT3 family (Fig. S1*C*). In vitro arginine methyltransferase assays showed that AtPRMT3 is a biochemically active methyltransferase, because it catalyzed the methylation of histones H3 and H4 of calf thymus core histones and methylation of myelin basic protein (Fig. S2). To investigate its intracellular distribution, we constructed an AtPRMT3 fusion to GFP, with the *AtPRMT3* full-length genomic DNA fused to *GFP-His* and transformed into *Arabidopsis* Col plants (Fig. S3 *A* and *B*). GFP fluorescence was mainly detected in the cytoplasm (Fig. S3*C*), in agreement with subcellular fractionation assays (Fig. S3*D*). The cytoplasmic localization of AtPRMT3 resembles that of its counterparts in fission yeast and animal (34, 35), indicating that AtPRMT3 may have conserved functions in the cytoplasm during evolution.

Disruption of *AtPRMT3* Confers Pleiotropic Developmental Defects Resembling Ribosome Biogenesis Mutants. To explore the biological functions of AtPRMT3 in vivo, we identified two independent transfer DNA (T-DNA) insertional mutants, designated *atprmt3-1* and *atprmt3-2*, with insertions located in the third exon

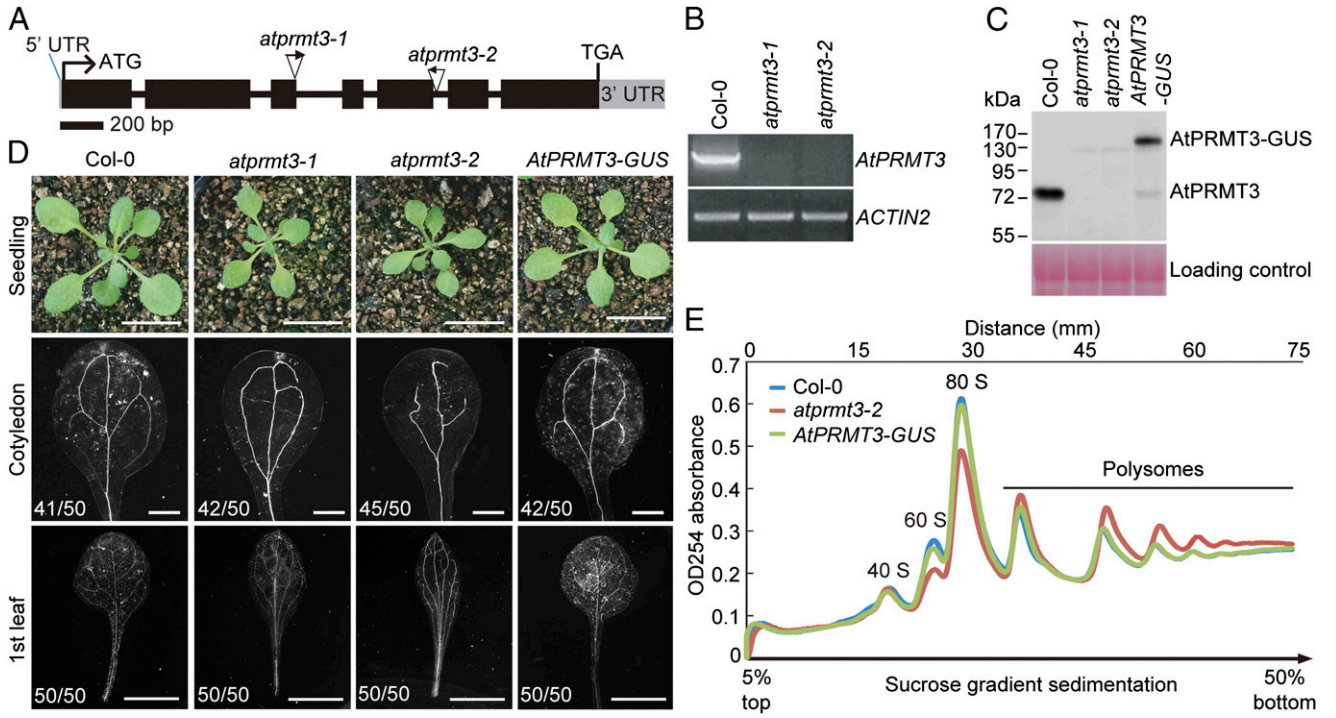

Fig. 1. Phenotypes of *atprmt3* null mutants. (*A*) The gene structure of *AtPRMT3* and locations of the T-DNA insertions in *atprmt3* mutants. (*B*) RT-PCR analysis of the full-length *AtPRMT3* transcript in wild-type Col and two *atprmt3* mutants (*Upper*). *Actin2* was used as an internal control (*Lower*). (*C*) Western blot analysis of AtPRMT3 protein in wild-type Col, *atprmt3* mutants, and the complemented line *AtPRMT3-GUS* (*Upper*). Rubisco large subunit stained with Ponceau S was used as an internal control (*Lower*). (*D*) *atprmt3* mutants exhibit an aberrant vein pattern in cotyledons and a typical pointed phenotype in the first true leaf. The numerator and denominator described in the figure represent the numbers of aberrant leaves and total leaves detected, respectively. [Scale bars, 10 mm for seedlings (*Upper*), 1 mm for cotyledons (*Middle*), 2 mm for the first true leaf (*Lower*).] (*E*) The polyribosome profile, monitored by absorbance at 254 nm over 5–50% sucrose gradient, in *atprmt3-2* shows down-regulation of the 60S large subunit and 80S monosome but up-regulation of polyribosomes.

PLANT BIOLOGY

and fifth intron of *AtPRMT3*, respectively (Fig. 1*A*). Both of them were null mutants, as confirmed by semiquantitative RT-PCR (Fig. 1*B*) and immunoblotting (Fig. 1*C*). The first true leaves of *atprmt3* mutant plants were narrow and pointed (Fig. 1*D*), and the adult leaves were serrated, compared with the round and regular shape of wild-type Col leaves (Fig. S4*A*). Furthermore, the *atprmt3* mutant leaves also showed distorted vascular patterns with more disconnected free ends (Fig. 1*D*). These leaf developmental defects are reminiscent of the *Arabidopsis* mutants of ribosome proteins (40) (Table S1), like S18A (also known as POINTED FIRST LEAF, *pfl* in its mutant) in the small subunit (41), or L4A and L4D in the large subunit (42). Moreover, null mutants of many nucleolus-localized ribosome assembly factors (Table S1), including the Pumilio-like RNA binding protein ARABIDOPSIS PUMILIO 23 (APUM23) (24), nucleolar RNA helicase ARABIDOPSIS MRNA TRANSPORT 4 (AtMTR4) (23), and a putative methyltransferase ROOT INITIATION DEFECTIVE 2 (RID2) (43), also display similar developmental defects and aberrant pre-rRNA processing. In addition to the leaf phenotypes, *atprmt3* mutants also displayed growth retardation, including delayed germination and primary root growth (Fig. S4 *B–D*). We also observed that approximately 13% of the flowers in *atprmt3-2* mutants show aberrant flower morphogenesis with five petals and five pistils, instead of the four petals and six pistils typical of wild-type plants (Fig. S4 *E* and *F*), a phenotype that resembles *rpl4a* and *rpl4d* mutants (42). All of these growth and developmental defects in *atprmt3-2* were complemented in the transgenic line *AtPRMT3-GUS*, which has a transgene with *AtPRMT3* fused to *GUS* (Fig. 1*D* and Fig. S4). These results suggest that *AtPRMT3* is indeed functional for normal growth and development in *Arabidopsis* and may play key roles in ribosome biogenesis.

***atprmt3* Mutants Show Aberrant Ribosomal Function.** The ribosome biogenesis mutants *apum23* and *rpl4* displayed varied sensitivity to translational inhibitors, as a result of putative aberrant ribosome structure and function (24, 42). Therefore, we evaluated the ribosomal function in *atprmt3* using antibiotics with known targets in the ribosome (44, 45). The *atprmt3* mutants exhibited marked resistance to several aminoglycoside antibiotics, including kanamycin, gentamicin, streptomycin, and spectinomycin (Fig. S5*A*), as well as hygromycin B (Fig. S5*B*), having longer roots than wild type or green cotyledons and leaves. These aminoglycoside antibiotics preferentially target the acceptor site (A site) in the ribosome during translation, change the allosteric control, disturb the decoding progress, and induce misreading, thereby slowing down translocation and translational elongation (46–48). All of these physiological defects were restored to wild-type levels in the complemented line *AtPRMT3-GUS* (Fig. S5 *A* and *B*). As controls, chloramphenicol prevents protein chain elongation by blocking peptidyl transferase activity, and tetracycline inhibits translation by disturbing the loading of aminoacylated tRNA (aa-tRNA) in the A site of the small subunit (44). The *atprmt3* seedlings displayed similar sensitivity to chloramphenicol and mild resistance to tetracycline compared with wild-type Col (Fig. S5*A*). These observations strongly suggest that *atprmt3* mutants may have altered ribosomal structure around the A site or have an aberrant population of ribosomes that were unable to bind aminoglycoside antibiotics properly.

To further determine the ribosome assembly state in vivo, we examined the polyribosome profile, detecting it by absorbance at 254 nm, after traditional biochemical purification of ribosomes and sucrose density gradient sedimentation. Compared with wild-type Col, the *atprmt3* mutants showed decreased ratios of 60S/40S and 80S/40S and increased ratios of polyribosomes (Fig. 1*E*). This imbalanced polysome profile was restored to wild type in *AtPRMT3-GUS* (Fig. 1*E*), indicating that AtPRMT3 participates in the ribosomal assembly in vivo.

PRMT3 Is Required for Proper Pre-rRNA Processing in *Arabidopsis*. During eukaryotic ribosome biogenesis, a polycistronic pre-rRNA transcript is processed into the mature 18S rRNA, 5.8S, and 25S/28S rRNAs, the key components of the 40S and 60S subunits, respectively (49). To explore whether AtPRMT3 participates in pre-rRNA processing, Northern blot analyses were performed to detect steady-state levels of pre-rRNA intermediates in each processing step. Null mutants of both *atprmt3-1* and *atprmt3-2* exhibited aberrant accumulation of an intermediate that was slightly shorter than 35S rRNA (red asterisk in Fig. S6), as detected by a DNA probe against the mature 25S

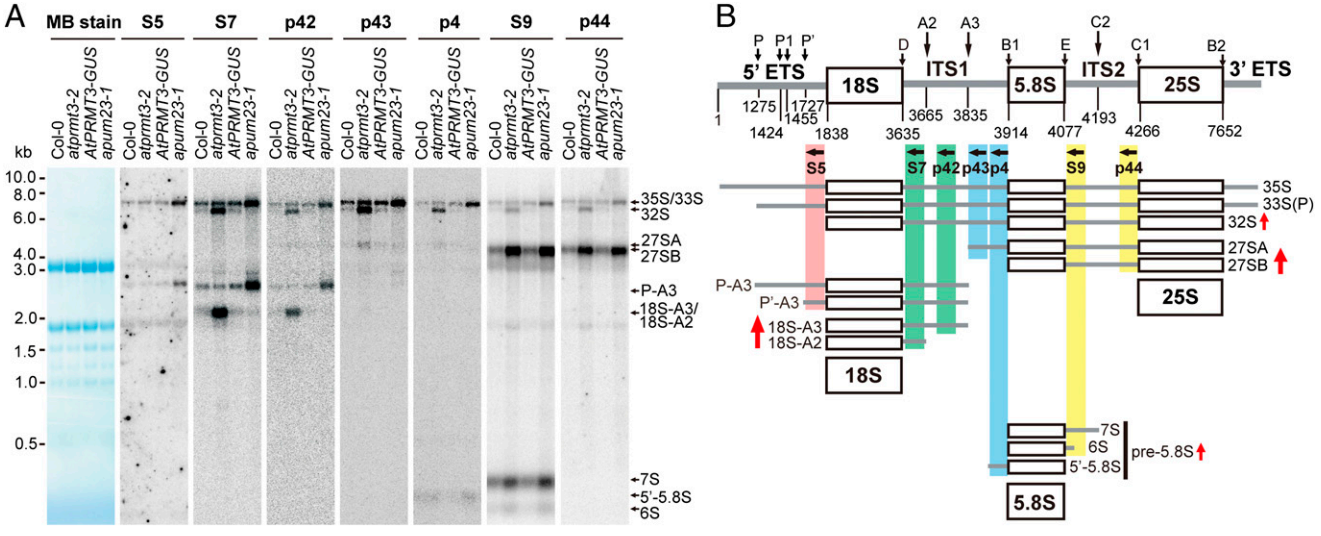

Fig. 2. Aberrant pre-rRNA processing in *atprmt3*. (*A*) Northern blots identified aberrant accumulation of 32S, 27S (27SA or 27SB), pre-18S (21S or 20S), and pre-5.8S (7S, 5′-5.8S and 6S) rRNAs in *atprmt3* mutants. *apum23-1* is a positive control accumulating 35S pre-rRNA and the P-A3 fragment. Methylene blue staining (MB stain) of a membrane is shown as a loading control. (*B*) Diagram illustrating the various pre-rRNA processing intermediates detected by Northern blots with specific probes, which are indicated by horizontal arrows. Black vertical arrows above the diagram indicate endonucleolytic cleavage sites relevant to this study. Red arrows indicate accumulated rRNA intermediates detected by Northern blot assays.

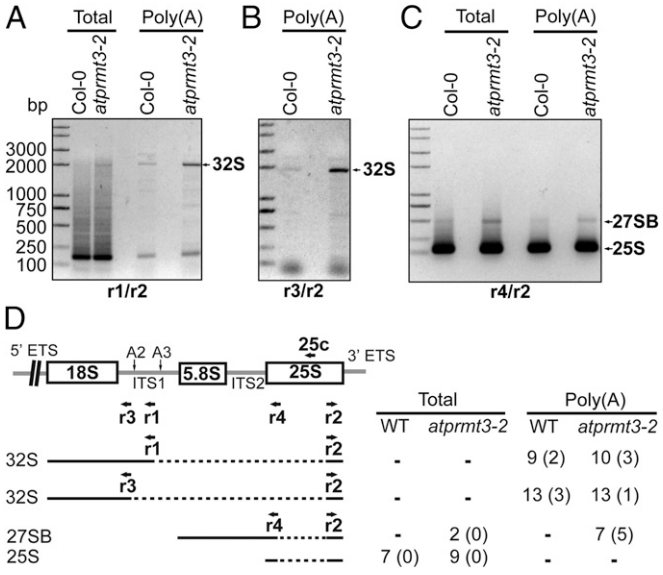

Fig. 3. Mapping of the 3′ and 5′ extremities of pre-rRNA by circular RT-PCR with cDNA reverse transcribed with the 25c primer. (*A* and *B*) Increased accumulation of 32S rRNA in *atprmt3-2* determined by PCR with r1/r2 (*A*) and r3/r2 primers (*B*). (*C*) Increased accumulation of 27SB intermediates in *atprmt3-2* checked by PCR with r4/r2 primers. Negative images of ethidium bromide-stained 1.5% (wt/vol) agarose gels are shown. (*A*–*C*) Sizes of DNA markers (bp) are indicated on the left in *A*. (*D*) The diagram illustrates the amplified PCR fragments. For each fragment, the number of clones obtained from wild-type and *atprmt3-2* samples is indicated on the right. The number of polyadenylated clones is marked in parentheses. –, no identification; Poly (A), template reverse transcribed from oligo-dT purified RNA; Total, template reverse transcribed from total RNA.

rRNA (Fig. S6 and Table S2). Then we focused on *atprmt3-2* and *AtPRMT3-GUS* for further Northern blot assays. We used *apum23-1* as a control mutant, because it shows aberrant accumulation of 35S and polyadenylated P-A3 pre-rRNAs (24). Probes used previously (22, 23) were able to detect the 35S and 33S precursors (Fig. 2 and Table S2). Probe S5, in the 5′ ETS, could distinguish the 35/33S precursors from the putative 32S rRNA. S7 and p42 in ITS1 could specifically detect the 18S precursors, including P-A3, P'-A3, 18S-A3, and/or 18S-A2 in the pre-40S small subunit. We used p43 and p4 in ITS1, and S9 and p44 in ITS2 to monitor the variations of 27S fragments (27SA and 27SB) and pre-5.8S rRNAs in the pre-60S large subunit (Fig. 2*B*). We found that pre-rRNA processing in *atprmt3-2* was relatively normal before the putative 32S rRNA (Fig. 2*A*). Intriguingly, pre-rRNA intermediates from the putative 32S rRNA in *atprmt3-2* showed strikingly aberrant accumulation (red arrow in Fig. 2*B*), including 18S-A3 and/or 18S-A2 in pre-40S small subunit and 27S fragments (mainly 27SB), as well as pre-5.8S rRNA in the pre-60S large subunit, respectively (Fig. 2*A*).

In addition, we also observed a sixfold increase in accumulation of the P-P1 byproduct in *atprmt3-2* (Fig. S7 *A* and *B*), most of which accumulated as the shorter version of 150 nt (Fig. S7*C*), indicating the defects in 5′ ETS processing or impaired degradation of rRNA maturation byproducts. Notably, all of these defects of pre-rRNA processing in *atprmt3-2* were recovered in *AtPRMT3-GUS* (Fig. 2 and Fig. S7) and were unique to *atprmt3* compared with other *Arabidopsis prmt* mutants reported previously (Fig. S8), demonstrating a specific and crucial role for AtPRMT3 in pre-rRNA processing and ribosome biogenesis.

An Alternative Pre-rRNA Processing Pathway Exists in *Arabidopsis* and Is Up-Regulated in *atprmt3* Mutants. Our Northern blot analysis showed detectable level and over-accumulation of the putative marker fragment 32S rRNA in Col-0 and *atprmt3-2* mutants, respectively (Fig. 2 and Fig. S8*A*). The 32S rRNA derives from complete removal of the 5′ ETS and is diagnostic for the U3 dependent cleavage occurs first pathway, the major pathway in budding yeast (17). To validate the increased abundance of 32S rRNA in *atprmt3* mutants (Fig. 2*A*), we performed circular RT-PCR with cDNA reverse transcribed by the 25c primer to determine the precise 3′ and 5′ ends of the pre-rRNA intermediates. Intact 32S rRNA (18S-ITS1-5.8S-ITS2-25S) was detected in wild-type and notably up-regulated in *atprmt3-2* (Fig. 3 *A*, *B*, and *D*), further confirming that an alternative pre-rRNA processing pathway also exists in *Arabidopsis*. Moreover, intact 27SB rRNA (5.8S-ITS2-25S) contributed more to 27S rRNA up-regulation in *atprmt3* mutants than 27SA (Fig. 3 *C* and *D*), as detected by probes S9 and p44 against ITS2 (Fig. 2).

AtPRMT3 Promotes the Major Pre-rRNA Processing Pathway Marked by the P-A3 Fragment. The 32S rRNA intermediate is the product of faster removal of 5′ ETS, or of delayed cleavage of ITS1 in A3. Its aberrant accumulation in *atprmt3* mutants may indicate varied processing dynamics between 5′ ETS and ITS1, representing the 5′ and 3′ terminus of the 18S rRNA, respectively. To further decipher the precise 5′ and 3′ extremities of pre-18S rRNAs, circular RT-PCRs were performed with cDNA reverse transcribed by the 18c RT primer (Fig. 4). Surprisingly, P-A3 and P'-A3, two pre-18S rRNAs of the major pre-rRNA processing pathway, were strikingly reduced, and 18S-A3 was over-accumulated in *atprmt3-2* mutants (Fig. 4 *A*–*C*). Additionally, 18S-A3 and 27SB were polyadenylated in *atprmt3* mutants (Figs. 3*D* and 4*D*), indicating potentially delayed processing of presmall subunit and prelarge subunit and activated polyadenylation-dependent RNA quality control in plants (9, 50).

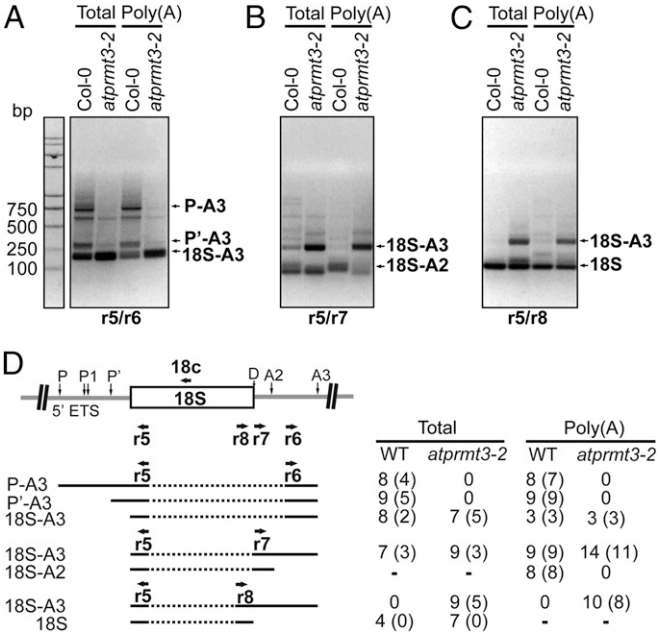

Fig. 4. Mapping of 3′ and 5′ extremities of pre-18S rRNAs by circular RT-PCR with cDNA reverse transcribed with the 18c primer. (*A*) Striking decrease of P-A3 intermediates in *atprmt3-2* checked by PCR with r5/r6 primers. (*B* and *C*) Significant increase of 18S-A3 intermediates in *atprmt3-2* validated by PCR with r5/r7 (*B*) and r5/r8 (*C*). (*D*) The diagram illustrates the amplified PCR fragments. For each fragment, the number of clones obtained from wild-type and *atprmt3-2* samples is indicated on the right. The number of polyadenylated clones is marked in parentheses. –, no identification; Poly(A), template reverse transcribed from oligo-dT purified RNA; Total, template reverse transcribed from total RNA.

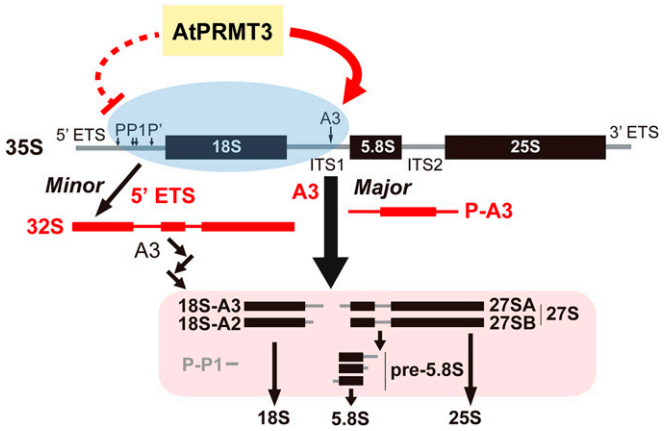

Fig. 5. Working model of AtPRMT3 in pre-rRNA processing. Two pre-rRNA processing pathways, which are different in cleavage order but not cleavage site, coexist in *Arabidopsis*. The P-A3 fragment and 32S rRNA are diagnostic for the major and minor pathways, respectively. AtPRMT3 in vivo promotes the major pathway and inhibits the minor pathway, probably by promoting the processing kinetics of site A3 in ITS1. Disruption of AtPRMT3 inhibits the A3 cleavage activity, causes unbalanced pre-rRNA processing pathways with down-regulation of the major pathway (P-A3) and up-regulation of the minor pathway (32S rRNA), and displays pre-rRNA processing defects as well as developmental phenotypes shared by ribosome biogenesis mutants.

We propose that two pre-rRNA processing pathways coexist in *Arabidopsis*, in which ITS1 cleavage occurs before or after complete removal of the 5′ ETS, respectively, as a result of uncoupled cleavage at A3 site and removal of 5′ ETS, which are processed via different kinetics (Fig. 5). In wild-type Col, cleavage at A3 site (major pathway) is so fast that the 32S rRNA from the 5′ ETS-first pathway (minor pathway) is rarely detectable (22–25). AtPRMT3 modulates the homeostasis between these pathways in vivo, probably mainly by promoting the cleavage kinetics at A3 site. Therefore, disruption of AtPRMT3 inhibits A3 cleavage and causes aberrant accumulation of the processing intermediates from the 5′ ETS-first pathway (Fig. 5).

Discussion

Our work provides genetic and biochemical evidence to demonstrate that AtPRMT3 plays a key role in ribosome biogenesis at the level of pre-rRNA processing, by modulating the balance between alternative pre-rRNA processing pathways, to promote plant growth and development.

Alternative pre-rRNA processing pathways exist widely in eukaryotes (51). The primary difference between these pathways is the order of 5′ ETS removal and ITS1 cleavage, other than the cleavage site (51). In *Arabidopsis*, the major pre-rRNA processing pathway corresponds to the minor pathway in budding yeast (17, 26) and the major pathway in *Xenopus* oocytes (18, 19), mouse cells, and human cells (20, 21). Here, we show the existence of 32S pre-rRNA in *Arabidopsis*, which underscores the conservation of alternative pre-rRNA processing. We propose that the balance between pre-rRNA processing pathways, as a result of uncoupled processing kinetics in both the A3 cleavage in ITS1 and 5′ ETS removal, is required for efficient pre-rRNA processing and normal growth and development, as well as adaptation to environmental changes. Thus, unbalanced pre-rRNA processing pathways in *atprmt3* mutants resulted in aberrant accumulation of rRNA maturation intermediates, which leads to abnormal ribosomal functions, producing varied responses to aminoglycoside antibiotics and altered polyribosome profiles. Furthermore, growth and developmental defects shared by *atprmt3* and other ribosome biogenesis mutants further emphasize the biological importance of proper pre-rRNA processing in higher plants (23, 24, 40, 43) (Table S1).

In eukaryotes, PRMTs regulate multiple biological processes, including DNA transcription, mRNA splicing, and piRNA biogenesis, but the link between PRMT and pre-rRNA processing has yet to be described (30, 31). In fission yeast, although PRMT3 balances the ratio of 40S and 60S free subunits for ribosome biogenesis, no pre-rRNA processing defect was reported (34). We find that *Arabidopsis* PRMT3 is required for proper pre-rRNA processing, thus to our knowledge providing the first evidence to demonstrate that PRMT can also function in post-transcriptional processing of rRNA to fine-tune ribosome biogenesis. We hypothesize that the distinct functions of PRMT3 in fission yeast and *Arabidopsis* may reflect the difference between unicellular and multicellular organisms. Thus, it will be informative to determine whether this regulatory mechanism is conserved in other higher eukaryotes.

AtPRMT3 is required for proper pre-rRNA processing and ribosome biogenesis, a role distinct from those of other, previously reported AtPRMTs (29). The null mutants of only *AtPRMT3*, but not *AtPRMT1a/1b* (52), *AtPRMT4a/4b* (53), *AtPRMT10* (39, 54), or *AtPRMT5* (55–59), display developmental phenotypes resembling those of ribosome biogenesis mutants (23, 24, 40, 43). *APUM23* encodes a pre-rRNA processing-related factor. Its null mutants show specific up-regulation of *AtPRMT3* but not other *AtPRMTs*, along with genes involved in ribosome biogenesis (24). These observations strongly suggest that AtPRMT3 specifically affects the pre-rRNA processing machinery. We speculate that the unique feature of the C2H2 zinc finger in the N terminus of AtPRMT3 may mediate this specific regulatory function. Cytoplasmic localization is another conserved feature of all reported PRMT3 proteins (28, 30) and AtPRMT3 described here. However, pre-rRNA processing mainly occurs in the nucleolus (60). We speculate that the arginine methylation substrates of AtPRMT3 or its direct binding partners may move into the nucleus to participate the pre-rRNA processing. It will be intriguing to decipher the signals that link AtPRMT3 in the cytoplasm to pre-rRNA processing in the nucleolus. Further exploration will uncover the gap between AtPRMT3 and pre-rRNA processing.

Materials and Methods

Plant Materials. The *atprmt3-1* (SAIL_220_F08) and *atprmt3-2* (WISCDSLOX391A01) mutants were obtained from the *Arabidopsis* Biological Resource Center. Further details can be found in *SI Materials and Methods*.

Polyribosome Profile Analysis and Sucrose Gradient Fractionation. Extracts were prepared for polyribosome profile analysis according to the method described before (61), with some modifications. A total of 5,000 A260 units of the resuspension was layered onto a linear 5–50% sucrose gradient poured with the Gradient Master 108 (BioComp Instruments) according to the user's manual, then ultracentrifuged in a Beckman SW-41Ti rotor at 213,669 × *g* for 3 h at 4 °C. The gradients were then analyzed from top to bottom, using the Piston Gradient Fractionator (BioComp Instruments) attached to the Model EM-1 Econo UV Monitor (BioRad) for continuous measurement of the absorbance at 254 nm. Further details can be found in *SI Materials and Methods*.

Northern Blot Analysis. Total RNA was isolated from 14-day-old seedlings using TRIzol reagent (TIANGEN, DP405-02) according to the manufacturer's instructions. Three micrograms of total RNA was separated on a 1.2% (wt/vol) agarose/formaldehyde gel or a 15% (wt/vol) acrylamide/7 M urea gel and transferred to a Hybond N+ membrane (GE Healthcare) by capillary elution or electrotransfer, respectively. The blots were washed and exposed to a storage phosphor screen (GE Healthcare), then signals were detected by the Typhoon TRIO scanner (GE Healthcare). A complete list of primers is provided in Table S2. Further details can be found in *SI Materials and Methods*.

Circular RT-PCR Assay. Circular RT-PCR analysis was carried out using 5 μg total RNA or 0.5 μg poly(A) RNA purified by a Dynabeads mRNA purification kit (Life Technologies, 61006) and was performed as previously described (24, 62). After amplification for 30 cycles, bands obtained by circular RT-PCR were cloned into the pEasy-T vector (TRANSGENE, CT101-02), and multiple clones were sequenced using M13F and/or M13R primers. Further details can be found in *SI Materials and Methods*.

Additional methods are available in *SI Materials and Methods*.

ACKNOWLEDGMENTS. We thank Dr. Sang-Bong Choi (Myongji University) for providing *apum23-1* seeds, the *Arabidopsis* Biological Resource Center for providing T-DNA insertion lines, and Dr. Lifang Niu for creating the pGEX-4T2-*AtPRMT3* construct. This work was supported by National Natural Science Foundation of China Grants 31330020, 31210103901 (to X.C.), and 31370770 (to C.L.), National Basic Research Program of China Grant 2011CB915401 (to X.C.), State Key Laboratory of Plant Genomics Grant 2011B0525 (to X.C.), and Chinese Academy of Sciences Grant KSCX2-EW-Q-24 (to C.L.).

1. Venema J, Tollervey D (1999) Ribosome synthesis in *Saccharomyces cerevisiae*. *Annu Rev Genet* 33:261–311.
2. Woolford JL, Jr, Baserga SJ (2013) Ribosome biogenesis in the yeast *Saccharomyces cerevisiae*. *Genetics* 195(3):643–681.
3. Warner JR (1999) The economics of ribosome biosynthesis in yeast. *Trends Biochem Sci* 24(11):437–440.
4. Lafontaine DL (2010) A 'garbage can' for ribosomes: How eukaryotes degrade their ribosomes. *Trends Biochem Sci* 35(5):267–277.
5. Tafforeau L, et al. (2013) The complexity of human ribosome biogenesis revealed by systematic nucleolar screening of Pre-rRNA processing factors. *Mol Cell* 51(4):539–551.
6. Ferreira-Cerca S, Pöll G, Gleizes PE, Tschochner H, Milkereit P (2005) Roles of eukaryotic ribosomal proteins in maturation and transport of pre-18S rRNA and ribosome function. *Mol Cell* 20(2):263–275.
7. Ferreira-Cerca S, et al. (2007) Analysis of the in vivo assembly pathway of eukaryotic 40S ribosomal proteins. *Mol Cell* 28(3):446–457.
8. Houseley J, LaCava J, Tollervey D (2006) RNA-quality control by the exosome. *Nat Rev Mol Cell Biol* 7(7):529–539.
9. Doma MK, Parker R (2007) RNA quality control in eukaryotes. *Cell* 131(4):660–668.
10. McCann KL, Baserga SJ (2013) Genetics. Mysterious ribosomopathies. *Science* 341(6148):849–850.
11. Narla A, Ebert BL (2010) Ribosomopathies: Human disorders of ribosome dysfunction. *Blood* 115(16):3196–3205.
12. Henras AK, et al. (2008) The post-transcriptional steps of eukaryotic ribosome biogenesis. *Cell Mol Life Sci* 65(15):2334–2359.
13. Osheim YN, et al. (2004) Pre-18S ribosomal RNA is structurally compacted into the SSU processome prior to being cleaved from nascent transcripts in *Saccharomyces cerevisiae*. *Mol Cell* 16(6):943–954.
14. Dragon F, et al. (2002) A large nucleolar U3 ribonucleoprotein required for 18S ribosomal RNA biogenesis. *Nature* 417(6892):967–970.
15. Grandi P, et al. (2002) 90S pre-ribosomes include the 35S pre-rRNA, the U3 snoRNP, and 40S subunit processing factors but predominantly lack 60S synthesis factors. *Mol Cell* 10(1):105–115.
16. Lee SJ, Baserga SJ (1997) Functional separation of pre-rRNA processing steps revealed by truncation of the U3 small nucleolar ribonucleoprotein component, Mpp10. *Proc Natl Acad Sci USA* 94(25):13536–13541.
17. Gallagher JE, et al. (2004) RNA polymerase I transcription and pre-rRNA processing are linked by specific SSU processome components. *Genes Dev* 18(20):2506–2517.
18. Savino R, Gerbi SA (1990) In vivo disruption of *Xenopus* U3 snRNA affects ribosomal RNA processing. *EMBO J* 9(7):2299–2308.
19. Peculis BA, Steitz JA (1993) Disruption of U8 nucleolar snRNA inhibits 5.8S and 28S rRNA processing in the *Xenopus* oocyte. *Cell* 73(6):1233–1245.
20. Bowman LH, Rabin B, Schlessinger D (1981) Multiple ribosomal RNA cleavage pathways in mammalian cells. *Nucleic Acids Res* 9(19):4951–4966.
21. Hadjiolova KV, Nicoloso M, Mazan S, Hadjiolov AA, Bachellerie JP (1993) Alternative pre-rRNA processing pathways in human cells and their alteration by cycloheximide inhibition of protein synthesis. *Eur J Biochem* 212(1):211–215.
22. Zakrzewska-Placzek M, Souret FF, Sobczyk GJ, Green PJ, Kufel J (2010) *Arabidopsis thaliana* XRN2 is required for primary cleavage in the pre-ribosomal RNA. *Nucleic Acids Res* 38(13):4487–4502.
23. Lange H, Sement FM, Gagliardi D (2011) MTR4, a putative RNA helicase and exosome co-factor, is required for proper rRNA biogenesis and development in *Arabidopsis* thaliana. *Plant J* 68(1):51–63.
24. Abbasi N, et al. (2010) APUM23, a nucleolar Puf domain protein, is involved in pre-ribosomal RNA processing and normal growth patterning in *Arabidopsis*. *Plant J* 64(6):960–976.
25. Missbach S, et al. (2013) 40S ribosome biogenesis co-factors are essential for gametophyte and embryo development. *PLoS ONE* 8(1):e54084.
26. Dunbar DA, Wormsley S, Agentis TM, Baserga SJ (1997) Mpp10p, a U3 small nucleolar ribonucleoprotein component required for pre-18S rRNA processing in yeast. *Mol Cell Biol* 17(10):5803–5812.
27. Liu C, Lu F, Cui X, Cao X (2010) Histone methylation in higher plants. *Annu Rev Plant Biol* 61:395–420.
28. Bedford MT, Clarke SG (2009) Protein arginine methylation in mammals: Who, what, and why. *Mol Cell* 33(1):1–13.
29. Ahmad A, Cao X (2012) Plant PRMTs broaden the scope of arginine methylation. *J Genet Genomics* 39(5):195–208.
30. Bachand F (2007) Protein arginine methyltransferases: From unicellular eukaryotes to humans. *Eukaryot Cell* 6(6):889–898.
31. Yang Y, Bedford MT (2013) Protein arginine methyltransferases and cancer. *Nat Rev Cancer* 13(1):37–50.
32. Ren J, et al. (2010) Methylation of ribosomal protein S10 by protein-arginine methyltransferase 5 regulates ribosome biogenesis. *J Biol Chem* 285(17):12695–12705.
33. Shin HS, et al. (2009) Arginine methylation of ribosomal protein S3 affects ribosome assembly. *Biochem Biophys Res Commun* 385(2):273–278.
34. Bachand F, Silver PA (2004) PRMT3 is a ribosomal protein methyltransferase that affects the cellular levels of ribosomal subunits. *EMBO J* 23(13):2641–2650.
35. Tang J, Gary JD, Clarke S, Herschman HR (1998) PRMT 3, a type I protein arginine N-methyltransferase that differs from PRMT1 in its oligomerization, subcellular localization, substrate specificity, and regulation. *J Biol Chem* 273(27):16935–16945.
36. Zhang X, Zhou L, Cheng X (2000) Crystal structure of the conserved core of protein arginine methyltransferase PRMT3. *EMBO J* 19(14):3509–3519.
37. Swiercz R, Cheng D, Kim D, Bedford MT (2007) Ribosomal protein rpS2 is hypomethylated in PRMT3-deficient mice. *J Biol Chem* 282(23):16917–16923.
38. Miyata S, Mori Y, Tohyama M (2010) PRMT3 is essential for dendritic spine maturation in rat hippocampal neurons. *Brain Res* 1352:11–20.
39. Niu L, Lu F, Pei Y, Liu C, Cao X (2007) Regulation of flowering time by the protein arginine methyltransferase AtPRMT10. *EMBO Rep* 8(12):1190–1195.
40. Byrne ME (2009) A role for the ribosome in development. *Trends Plant Sci* 14(9):512–519.
41. Van Lijsebettens M, et al. (1994) An S18 ribosomal protein gene copy at the *Arabidopsis* PFL locus affects plant development by its specific expression in meristems. *EMBO J* 13(14):3378–3388.
42. Rosado A, et al. (2010) Auxin-mediated ribosomal biogenesis regulates vacuolar trafficking in *Arabidopsis*. *Plant Cell* 22(1):143–158.
43. Ohbayashi I, Konishi M, Ebine K, Sugiyama M (2011) Genetic identification of *Arabidopsis* RID2 as an essential factor involved in pre-rRNA processing. *Plant J* 67(1):49–60.
44. Spahn CM, Prescott CD (1996) Throwing a spanner in the works: Antibiotics and the translation apparatus. *J Mol Med (Berl)* 74(8):423–439.
45. Yonath A (2005) Antibiotics targeting ribosomes: Resistance, selectivity, synergism and cellular regulation. *Annu Rev Biochem* 74:649–679.
46. Brodersen DE, et al. (2000) The structural basis for the action of the antibiotics tetracycline, pactamycin, and hygromycin B on the 30S ribosomal subunit. *Cell* 103(7):1143–1154.
47. Carter AP, et al. (2000) Functional insights from the structure of the 30S ribosomal subunit and its interactions with antibiotics. *Nature* 407(6802):340–348.
48. Tsai A, et al. (2013) The impact of aminoglycosides on the dynamics of translation elongation. *Cell Reports* 3(2):497–508.
49. Fatica A, Tollervey D (2002) Making ribosomes. *Curr Opin Cell Biol* 14(3):313–318.
50. Lange H, Sement FM, Canaday J, Gagliardi D (2009) Polyadenylation-assisted RNA degradation processes in plants. *Trends Plant Sci* 14(9):497–504.
51. Mullineux ST, Lafontaine DL (2012) Mapping the cleavage sites on mammalian pre-rRNAs: Where do we stand? *Biochimie* 94(7):1521–1532.
52. Yan D, Zhang Y, Niu L, Yuan Y, Cao X (2007) Identification and characterization of two closely related histone H4 arginine 3 methyltransferases in *Arabidopsis thaliana*. *Biochem J* 408(1):113–121.
53. Niu L, Zhang Y, Pei Y, Liu C, Cao X (2008) Redundant requirement for a pair of PROTEIN ARGININE METHYLTRANSFERASE4 homologs for the proper regulation of Arabidopsis flowering time. *Plant Physiol* 148(1):490–503.
54. Niu L, Lu F, Zhao T, Liu C, Cao X (2012) The enzymatic activity of *Arabidopsis* protein arginine methyltransferase 10 is essential for flowering time regulation. *Protein Cell* 3(6):450–459.
55. Zhang Z, et al. (2011) *Arabidopsis* floral initiator SKB1 confers high salt tolerance by regulating transcription and pre-mRNA splicing through altering histone H4R3 and small nuclear ribonucleoprotein LSM4 methylation. *Plant Cell* 23(1):396–411.
56. Sanchez SE, et al. (2010) A methyl transferase links the circadian clock to the regulation of alternative splicing. *Nature* 468(7320):112–116.
57. Hong S, et al. (2010) Type II protein arginine methyltransferase 5 (PRMT5) is required for circadian period determination in *Arabidopsis thaliana*. *Proc Natl Acad Sci USA* 107(49):21211–21216.
58. Deng X, et al. (2010) Arginine methylation mediated by the *Arabidopsis* homolog of PRMT5 is essential for proper pre-mRNA splicing. *Proc Natl Acad Sci USA* 107(44):19114–19119.
59. Pei Y, et al. (2007) Mutations in the Type II protein arginine methyltransferase AtPRMT5 result in pleiotropic developmental defects in *Arabidopsis*. *Plant Physiol* 144(4):1913–1923.
60. Pendle AF, et al. (2005) Proteomic analysis of the *Arabidopsis* nucleolus suggests novel nucleolar functions. *Mol Biol Cell* 16(1):260–269.
61. Mustroph A, Juntawong P, Bailey-Serres J (2009) Isolation of plant polysomal mRNA by differential centrifugation and ribosome immunopurification methods. *Methods Mol Biol* 553:109–126.
62. Pfalz J, Bayraktar OA, Prikryl J, Barkan A (2009) Site-specific binding of a PPR protein defines and stabilizes 5′ and 3′ mRNA termini in chloroplasts. *EMBO J* 28(14):2042–2052.